Water Resources Research

RESEARCH ARTICLE
10.1029/2023WR035004

Special Section:
Quantifying human interferences in hydrologic process modeling

Key Points:

- Groundwater-fed irrigation increases mean evapotranspiration (*ET*) value and decreases relative variability (coefficient of variance)
- *ET* spatial patterns are characterized by irrigation heterogeneity and the natural east-to-west gradient in terrain and precipitation
- Correspondence between the transition of *ET* (mean vs. variability) and that of crop yield characterizes sustainable irrigation development

Supporting Information:

Supporting Information may be found in the online version of this article.

Correspondence to:
R. Zeng,
ruijie.zeng.1@asu.edu

Citation:
Zeng, R., Yao, C., Cai, X., & Haacker, E. (2023). Temporal and spatial pattern change in evapotranspiration over the High Plains: The impact of and guide on extensive groundwater-fed irrigation. *Water Resources Research*, *59*, e2023WR035004. https://doi.org/10.1029/2023WR035004

Received 30 MAR 2023
Accepted 23 NOV 2023

Author Contributions:
Conceptualization: Ruijie Zeng
Data curation: Chuncheng Yao, Erin Haacker
Formal analysis: Ruijie Zeng, Ximing Cai, Erin Haacker
Funding acquisition: Ruijie Zeng
Investigation: Ruijie Zeng, Erin Haacker
Methodology: Ruijie Zeng
Project Administration: Ruijie Zeng

Temporal and Spatial Pattern Change in Evapotranspiration Over the High Plains: The Impact of and Guide on Extensive Groundwater-Fed Irrigation

Ruijie Zeng[1], Chuncheng Yao[1], Ximing Cai[2], and Erin Haacker[3]

[1]School of Sustainable Engineering and the Built Environment, Arizona State University, Tempe, AZ, USA, [2]Ven Te Chow Hydrosystems Laboratory, Department of Civil and Environmental Engineering, University of Illinois at Urbana-Champaign, Champaign, IL, USA, [3]Nebraska Water Center, University of Nebraska-Lincoln, Lincoln, NE, USA

Abstract Aquifer depletion due to extensive and intensive irrigation in the High Plains has threatened the environmental sustainability of the region. The change of crop evapotranspiration (*ET*), the major form of agriculture water consumption, presents a critical signature of hydrologic cycle change. This study evaluates the relative contributions of climate and groundwater-fed irrigation to *ET* temporal and spatial pattern change over the High Plains Aquifer, one of the most severely depleted aquifers in the US. We developed a framework to extend the Budyko hypothesis to assess the impact of catchment storage change on long-term *ET*. It is found that irrigation from groundwater pumping contributes more than half of the increase in *ET* (74.1 mm) from the period of 1940–1975 to 1976–2010, despite an increase of precipitation (35.0 mm) in the region. *ET* seasonal variance is decreased by the decline in precipitation variability (at −20.7 mm) and increase in irrigation (at +14.2 mm). As expected, irrigation decreases *ET* coefficient of variability (i.e., the ratio of standard deviation to mean). Spatially, we find that the human-induced *ET* heterogeneity post-1975 superimposes over the natural east-to-west gradient (in precipitation and *ET*) of this region. A correlation between the statistics (mean vs. coefficient of variation) on *ET* and crop yield provides promising signatures for understanding the coupled natural and human system of High Plains agriculture. Guides are discussed regarding how to handle the tradeoffs between agricultural development and natural resource sustainability under climate variability in the High Plains and other regions with similar conditions.

1. Introduction

Crop production depends on massive groundwater-fed irrigation in many places around the world. Groundwater provides relatively stable water sources, especially in arid and semi-arid regions; however, over-exploitation of groundwater resources has been recognized as a major concern in sustainable regional development (Aeschbach-Hertig & Gleeson, 2012; Famiglietti, 2014; Konikow, 2011; Scanlon, Faunt, et al., 2012). The Republican River Basin, located in the Northern High Plains and comprising parts of Nebraska, Colorado, and Kansas, provides an outstanding example of how intensive groundwater irrigation effects propagate to hydrologic change, ecological deterioration and water rights conflicts (McGuire, 2014). Since the 1960s, the widespread adoption of central pivot irrigation systems has gradually caused groundwater depletion and reduced stream flow in the Republican River. In 1998, the downstream state Kansas sued upstream states Nebraska and Colorado in the Supreme Court for violating surface water rights due to the over-pumping of groundwater (Popelka, 2004). Other river basins in the High Plains are facing similar environmental issues and water rights conflicts due to extensive irrigation development. At the global scale, many other regions, such as California's Central Valley (Scanlon, Longuevergne, & Long, 2012), the North China Plain (Liu et al., 2008), India (Rodell et al., 2009) and the Middle East (Joodaki et al., 2014), have experienced similar situations of irrigation development and aquifer depletion. As seen in the above examples, human interferences are impacting hydrologic systems; water resource management will increasingly require scientific understanding of human impacts on hydrologic systems as future water needs change due to socioeconomic development and climate change.

Many studies have been conducted to understand groundwater depletion (Haacker et al., 2016; McGuire, 2014; Scanlon, Longuevergne, & Long, 2012; Strassberg et al., 2009) and streamflow changes (Burt et al., 2002; Szilagyi, 2001; Zeng & Cai, 2014) in the High Plains. The High Plains sit on the Ogallala Aquifer, one of the most productive aquifers in the Contingous United States (CONUS), which however is also seriously depleted (Dieter & Maupin, 2017; Hornbeck & Keskin, 2014). The accumulative depletion of groundwater in this region

Supervision: Ruijie Zeng
Validation: Ruijie Zeng, Chuncheng Yao
Writing – original draft: Ruijie Zeng
Writing – review & editing: Ruijie Zeng, Ximing Cai, Erin Haacker

during 1900–2008 is equivalent to 1 mm sea level rise (Konikow, 2011). Scanlon, Faunt, et al. (2012) estimated that if current groundwater withdrawal is continued, about 35% of the southern High Plains will be unable to support irrigation within the next 30 years.

However, the impacts of irrigation on the temporal and spatial pattern of evapotranspiration (*ET*) change in the region are not well documented. *ET* represents the major water consumption in the region, especially for agricultural water use, as argued by some studies that water resources management is essentially "*ET* management" (Foster & Garduño, 2004). Meanwhile, *ET* connects land surface energy and water budgets, driven by both climatic and anthropogenic forcings. A comprehensive assessment of the patterns of *ET* change is essential, on one hand to understand the human interferences to the hydrologic cycle retrospectively, and on the other hand to design regional sustainable water resources management.

However, limited *ET* observation and simulation prevent a comprehensive understanding of human induced change over a large temporal span and spatial extent, such as the High Plains (Figure S2 in Supporting Information S1). In particular, the number of groundwater wells in this region grew substantially beginning in the late 1950s (Mutiibwa & Irmak, 2013) and even as early as 1930s in parts of the Southern High Plains (Green, 1981), while *ET* estimates from remote sensing products are available only after the 1980s (Szilagyi & Franz, 2020; Wei et al., 2022). Furthermore, land surface models simulate irrigation as a result of soil moisture conditions (Lawston et al., 2015; Ozdogan et al., 2010), either neglecting anthropogenic forcings (e.g., pumping volume) or using estimates subject to significant bias and uncertainty (Demissie et al., 2015; Rossman & Zlotnik, 2013). Therefore, there is a lack of "pre-development" *ET* conditions as a baseline to evaluate the hydrologic change caused by groundwater-fed irrigation in this region.

This study provides a quantitative framework to assess *ET* temporal and spatial changes using long-term climate data and water table observations in the High Plains. To understand human interferences to *ET* processes and diagnose the climatic and anthropogenic factors to *ET* changes, the framework is established in the context of a coupled human and natural system (CHNS) (Liu et al., 2007). Questions to address include: (a) What are the changes of *ET* temporal characteristics (i.e., mean and seasonal variability) due to groundwater-fed irrigation in the High Plains? (b) What spatial changes have irrigation practices imposed upon the natural hydroclimatic gradient in the region? (c) How are the *ET* change patterns related to farmers' behaviors in balancing crop production profit and risk aversion? As irrigation has becomes the driving force for crop yield generation in this region, will the changes in hydro-climatic variables manifest themselves in the change of anthropogenic variables (e.g., crop yield)? Answers to these questions are also expected to provide a predictive understanding to what may happen in other regions that have experienced similar challenges.

2. Data and Methods

2.1. Impacts of Irrigation on Long-Term *ET*

The original Budyko's hypothesis prescribes a functional relation between *ET* and the two climate variables, precipitation (*P*) and potential evaporation (*PET*). The basin wide annual average *ET* is determined by the long-term climate conditions expressed as:

$$ET = f(P, PET) \tag{1}$$

There are several different parametric and non-parametric forms for the expressions of *f* (Fu, 1981; Yang et al., 2008). In this study, we adopt the expression from Yang et al. (2008):

$$ET = \frac{P \times PET}{(P^n + PET^n)^{1/n}} \tag{2}$$

Here, we developed a method to extend Budyko's hypothesis to calculate annual mean *ET* by explicitly incorporating the impact of groundwater storage change due to agricultural irrigation. As extensive groundwater is "mined" to provide irrigation to support agricultural evapotranspiration, catchment-storage change ΔS cannot be neglected in the water-budget balance, even on the long-term scale. For each time period *i* (e.g., year or month), the basin-wide water balance is

$$\Delta S_i = P_i - ET_i - Q_i \tag{3}$$

where Q is the net discharge across basin boundary. During irrigation season, the total available water $P_i' = P_i - \Delta S_i = ET_i + Q_i$ includes precipitation and complementary water supply from aquifer pumping. As ΔS_i is negative due to pumping induced catchment storage depletion, increased total water availability P_i' is partitioned between ET and runoff Q (including natural runoff and irrigation return flow). During non-irrigation season, aquifer storage recovers from recharge (i.e., ΔS_i is positive) and there is less water available for ET and runoff. Explicitly considering catchment storage change allows us to incorporate complete water balance (e.g., pumping from aquifer) in each time period into Budyko's energy-water partitioning.

Following Han et al. (2011) and Zeng and Cai (2015), we replaced the P in Equation 1 by P'. By applying Budyko curve in Equation 1 for each time periods, the basin wide evapotranspiration is

$$ET_i = f\left(P_i', PET_i\right) = f(P_i, PET_i, \Delta S_i) \tag{4}$$

The ET_i can be expressed as deviation from the long-term average $\overline{ET}$ from the Taylor expansion of Equation 4 near long-term climate condition $\left(\overline{P}, \overline{PET}\right)$ in Equation A1 in Appendix A.

Taking the expected value of ET_i in Equation A1, and noticing $E(P_i) = \overline{P}$, $E(PET_i) = \overline{PET}$, $E(\Delta S_i) = \overline{\Delta S}$, the long-term average ET is:

$$\begin{aligned}\overline{ET} = f\left(\overline{P}, \overline{PET}, \overline{\Delta S}\right) \\ + \frac{1}{2}\left[f_P''\sigma_P^2 + f_{PET}''\sigma_{PET}^2 + f_{\Delta S}''\sigma_{\Delta S}^2 + 2f_{P,\Delta S}''Cov(P, \Delta S)\right. \\ \left. + 2f_{PET,\Delta S}''Cov(PET, \Delta S) + 2f_{P,PET}''Cov(P, PET)\right]\end{aligned} \tag{5}$$

where $Var(X) = E\left[\left(X - \overline{X}\right)^2\right]$ and $Cov(X, Y) = E[(X - \overline{X})(Y - \overline{Y})]$ denote the variance and covariance, respectively. The expressions (Equation A2 in Appendix A) of the second order derivatives (i.e., $f_{X,Y}''$) in Equation 5 present the contributions of climate variability and catchment storage variation to long-term ET.

Equation 5 is an extension to the original Budyko curve and states that the long-term average ET (i.e., $\overline{ET}$) depends is affected by (a) long-term climatic conditions (i.e., the $f\left(\overline{P}, \overline{PET}, \overline{\Delta S}\right)$ term); (b) climate variability (e.g., seasonality, represented by represented by the variance/covariance terms $f_P''\sigma_P^2 + f_{PET}''\sigma_{PET}^2 + 2f_{P,PET}''Cov(P, PET)$); (c) catchment dynamic responses to climate (e.g., vegetation water use and groundwater change, represented by the variance/covariance terms $f_{\Delta S}''\sigma_{\Delta S}^2 + 2f_{P,\Delta S}''Cov(P, \Delta S) + 2f_{PET,\Delta S}''Cov(PET, \Delta S)$), and (d) catchment static characteristics (e.g., slope, soil type, vegetation type, represented by the parameter in Budyko equations as studied in Yang et al. (2007) and Zhang et al. (2001)). If the long-term catchment storage change is negligible (i.e., $\overline{\Delta S} = 0$) and ignoring the climate variability and catchment storage dynamics, Equation 5 reduces to the original Budyko equation in Equation 1.

We further applied Equation 5 to evaluate the contribution of climate seasonality (e.g., in-phase and out-of-phase between P and PET) and catchment storage change (e.g., snow and soil moisture) on long-term ET for watersheds in US detailed. In this study, we use Equation 5 to explicitly consider the impacts from pumping induced catchment storage change on ET over the High Plains. The empirical parameter n (in Equation 2 and Equation 5) is fixed at 1.58 for all sub-basins by fitting points on the Budyko curve with ET estimated as the differences between P and runoff with records during 1945–1970 (pre-development condition). It is noted that some studies fitted a time-varying parameter in the Budyko curve based on water balance data in different time periods, and attributed vegetation's dynamic control on ET to the parameter. Based on our experience, the calculated (rather than calibrated) parameter in Budyko curve suffers from the water budget error (especially the estimation of catchment storage ΔS) during each time period. Instead, this study represents catchment dynamic control (e.g., vegetation dynamics, subsurface water storage change) on ET through the variance/covariance terms related to ΔS in Equation 5 and catchment static controls through the empirical parameter of the Budyko curve. Therefore, the empirical parameter can also be estimated from the static catchment prosperities (Yang et al. (2007); Zhang et al. (2001)).

2.2. Impacts of Irrigation on Seasonal *ET* Variability

The *ET* variability is calculated based on the Evapotranspiration Temporal VARiance Decomposition (ETVARD) framework (Zeng & Cai, 2015, 2016):

$$\sigma_{ET}^2 = w_P\sigma_P^2 + w_{PET}\sigma_{PET}^2 + w_{\Delta S}\sigma_{\Delta S}^2 + w_{P,PET}cov_{P,PET} + w_{P,\Delta S}cov_{P,\Delta S} + w_{PET,\Delta S}cov_{PET,\Delta S} \quad (6)$$

where the *ET* temporal variance (σ_{ET}^2, at seasonal scale in this study) is decomposed into components from climatic fluctuations (i.e., σ_P^2 and σ_{PET}^2), seasonality between water and energy supply (i.e., $cov_{P,PET}$), groundwater storage variation (i.e., $\sigma_{\Delta S}^2$), and the responses of groundwater storage change to climate (i.e., $cov_{P,\Delta S}$ and $cov_{PET,\Delta S}$). The weighting factors (w), quantifying the contribution from each source to σ_{ET}^2, are derived from the sensitivity of *ET* to land surface moisture or energy constraints based on the long-term climatic conditions (i.e., the aridity index from long-term average *PET/P* and the derivatives in Budyko curve in Zeng and Cai (2015)). When farmers respond to low rainfall with groundwater-fed irrigation, the activity is captured via strong correlation between *P* and *ΔS*. At the same time, the arid and semi-arid climate condition yields a high value of weight $w_{P,\Delta S}$, which also reflects the irrigation impact via terrestrial storage change. Therefore, Equation 6 can be used to quantify the contribution attributed to both climatic and storage change factors (especially via irrigation in this study). The function forms for the six weight factors and detailed discussion for σ_{ET}^2 under the various climate and storage change conditions are documented in Zeng and Cai (2015).

ET temporal variability exhibits different magnitudes and contains different components depending on the time scale (e.g., annual, seasonal and monthly) (Zeng & Cai, 2016). This study focuses on *ET* temporal variability at the seasonal scale (i.e., crop growing season from May to October and non-growing season from November to April) for two reasons. First, in the crop growing season, aquifer water storage change is the main source of terrestrial water storage change; while other forms of water storage change such as soil moisture and snow cover are negligible. In addition, direct observations on soil moisture are not available for any large spatial extent and temporal span, and soil moisture from land surface model simulations may suffer from significant bias and uncertainty as irrigation is not well represented in existing *ET* models. Second, agricultural pumping is a seasonal event, and its impacts on *ET* patterns conform with a seasonal scale.

2.3. Climatic and Hydrologic Data

Monthly climate data from 1940 to 2010, including *P*, maximum temperature and minimum temperature, were obtained from PRISM Climate Group with a spatial resolution of 30 arcsec (~800 m) (Daly et al., 2008). *PET* is calculated from the Hargreaves temperature-based method (Hargreaves & Samani, 1982). The temperature based *PET* is further adjusted by *PET* calculated from a modified Penman scheme (Mahrt & Ek, 1984) in the North American Land Data Assimilation System-2 (NLDAS-2) from 1980 to 2010. With annual *P* ranging from 328 to 830 mm and annual *PET* from 995 to 1538 mm, the High Plains have an arid or semi-arid climate, where the aridity index (i.e., *PET/P*) varies between 1.4 and 4.7. The monthly *P* and *PET* are aggregated to seasonal scale for later calculation.

The water table change is interpolated from groundwater well measurements over the Ogallala Aquifer by ordinary kriging and the interpolation converted to a raster at a resolution of 250 m, following methods detailed in Haacker et al. (2016). On average, about 12,000 measurements in each season are used for spatial interpolation. In addition, elevations from 1984 stream locations are incorporated to filter out the interpolated water table values that are above the terrain surface. Note that the observed groundwater table change captures the net change of aquifer storage caused by both vertical and lateral fluxes, such as pumping, recharge, groundwater regional flow and baseflow discharge. Since most of the regional aquifer is unconfined, the water table change is multiplied by specific yield (Gutentag, 1984; McGuire et al., 2012) to obtain the aquifer water storage change (*ΔS*), which is calculated for both growing season (i.e., May to October when pumping wells are active) and non-growing season in this study.

Furthermore, to account for the hydroclimatic and anthropogenic heterogeneity, the USGS hydrologic unit code (HUC) 1:250000-scale Hydrologic Units (HUC250k) map (Seaber et al., 1987) is used to delineate the High Plains overlaying with the Ogallala Aquifer into 120 sub-basins. The PRISM climate data and USGS groundwater storage change are aggregated to the sub-basin level based on HUC250k boundary.

We also collected streamflow data from all 212 USGS streamflow gauges within the High Plains. The gauge stations have varying record lengths, and we included 178 gauges with records before 1975. It is noted that the USGS gauges may record streamflow from several HUC250K sub-basins, since some sub-basins are nested.

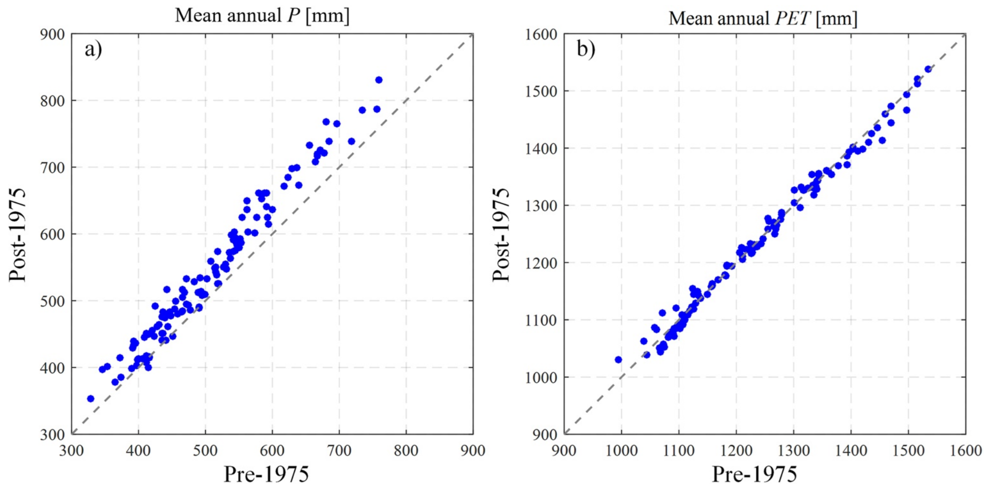

Figure 1. Mean annual (a) *P* and (b) *PET* of the 120 sub-basins in the High Plains during pre-1975 and post-1975 periods.

The 70-year (1940–2010) seasonal time series of *P*, *PET* and Δ*S* are divided into two periods (i.e., pre-1975 and post-1975, with the equal length for both periods) to calculate *ET* mean and temporal variance, respectively. For the long-term average in each period, we calculate mean annual *ET* using the long-term average hydroclimatic data (i.e., $\overline{P}$, $\overline{PET}$, $\overline{\Delta S}$) and the contributions from temporal variability terms in Equation 5. The *ET* seasonal variances are calculated by Equation 6. It is noted that large scale groundwater-fed irrigation development in this region occurred at different periods in this region, ranging from 1930s in the South High Plains and 1970s in the North High Plains (Haacker et al., 2016; McGuire, 2009; Scanlon, Faunt, et al., 2012). Although the two periods (pre-1975 and post-1975) are not accurately referred to “pre-development” and “development” conditions, the degree of intensive and extensive groundwater pumping after 1975 provides a comparative case of human interferences on *ET* patterns.

3. Results

3.1. *ET* Mean Change Over the High Plains

Using the 1940–1975 “pre-development” period as baseline, the annual *PET* remains unchanged (Figure 1b). Most of the sub-basins have increased *P* (35.0 mm on average) (Figure 1a) in the post-1975 period.

Most of the sub-basins yield a greater mean *ET* post-1975 than pre-1975, as shown in Figure 1a. While *ET* is expected to increase as *P* increases in the semi-arid High Plains, it is also possible that the enhanced *ET* from groundwater irrigation contributed to the increase of *P* especially during growing seasons.

The average annual *ET* in the 120 sub-basins increases by 74.1 mm from 399.6 mm pre-1975 to 473.7 mm post-1975, and the *ET* increase is more than 100 mm in some sub-basins (Figure 2a). Therefore, *P* alone cannot

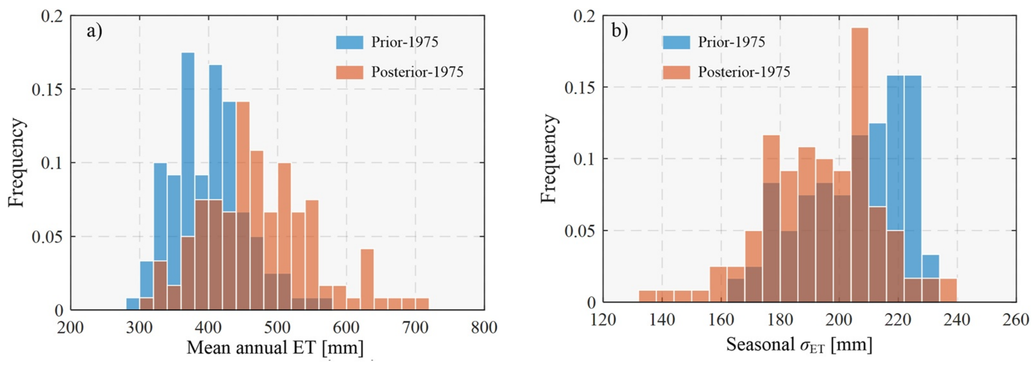

Figure 2. Histogram of (a) mean annual and (b) seasonal standard deviation of *ET* pre-1975 and post-1975 in 120 sub-basins over the High Plains.

10.1029/2023WR035004

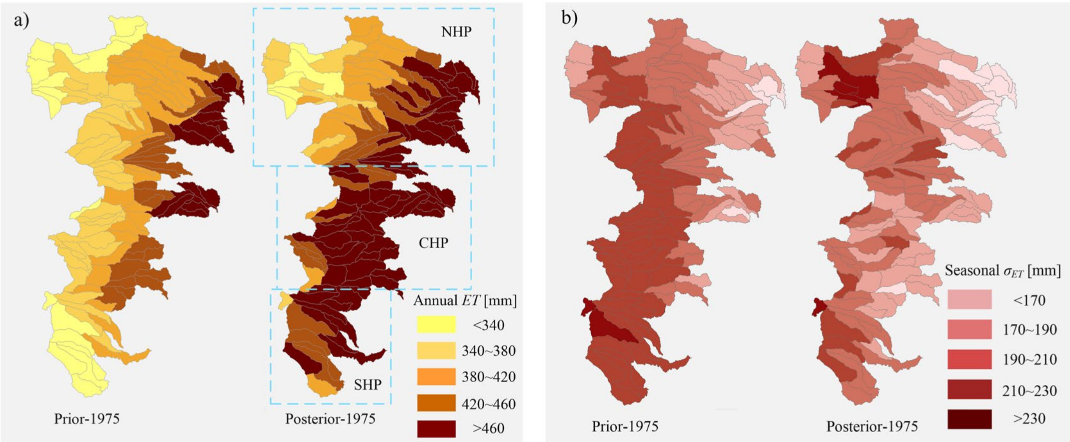

Figure 3. The spatial pattern of ET (a) mean annual and (b) seasonal standard deviation in 120 sub-basins over the High Plains.

fully explain the ET increase, even if all increased P is partitioned into ET. Therefore, irrigation from groundwater pumping contributes to at least more than half of the ET increase. We also checked all USGS gauging stations in this region with at least 10-year length records pre-1975 and found mixed changes in streamflow. More interesting, some gauging stations show increased streamflow during growing season and decreased streamflow during non-growing season. This change pattern may be caused by irrigation return flow from upstream (mainly happening in growing season) and stream depletion by long-term groundwater decline trend. Streamflow change due to irrigation shows both local (e.g., surface water withdrawal, stream depletion by nearby pumping well) and non-local (e.g., irrigation return flow in the upstream) impact of human activities. Therefore, the more detailed studies in this region should focused on the spatial and temporal patterns of streamflow change in this region (Szilagyi, 1999; Wen & Chen, 2006; Zipper et al., 2018).

Spatially, the average ET exhibits a clear east-to-west gradient pre-1975 as captured by the left map of Figure 3a. ET is relatively large in sub-basins in the east and small in the west, following the P gradient. Under significant irrigation practices post-1975, the east-to-west gradient in ET is no longer obvious in the Central High Plains (CHP) and the Southern High Plains (SHP). The increase of mean annual ET is consistent with the groundwater depletion map. As shown in the right map of Figure 3a, most areas of the CHP and the north part of the SHP show a significant ET increase. These regions also experienced the most significant decline in water table (Haacker et al., 2016; McGuire, 2014; Scanlon, Faunt, et al., 2012). In the Northern High Plains (NHP), ET increases are mainly located in the Republican River Basin and Lower Platte River Basin, while ET in the Upper Platte River Basin and the Sand Hills region has little change since agricultural development in these regions is not intensive due to the sandy soils (Istanbulluoglu et al., 2012; Wang et al., 2009). Therefore, the ET east-to-west gradient remains in the NHP without significant anthropogenic interferences.

3.2. *ET* Seasonal Variability Due To Irrigation

The seasonal σ_{ET} decreases from 205.3 mm pre-1975 to 193.6 mm post-1975 on average, and the change can be attributed to climate and storage components according to ETVARD by Equation 6. On one hand, some sub-basins experience damping in climatic fluctuation, which contributes to the decrease of σ_{ET} by 20.7 mm on average, as shown in Figure S1a in Supporting Information S1. The damping in climatic seasonal variability is mainly due to a more stable P in the region, since PET variability remains almost unchanged. On the other hand, the storage components in σ_{ET} increases by 14.2 mm on average as shown in Figure S1b in Supporting Information S1, especially in sub-basins in CHP and SHP with significant amount of groundwater pumping. Therefore, the decline in the total σ_{ET} results from the combined effects of less variance in P and larger variance in the storage components due to irrigation pumping. In terms of absolute values, the climatic components and storage components account for 59% and 41% change in σ_{ET}, respectively.

The ET seasonal variance also followed an east-to-west gradient pre-1975 as illustrated in the left map of Figure 3b, where the arid sub-basins in the west exhibit higher ET variability than those relatively humid

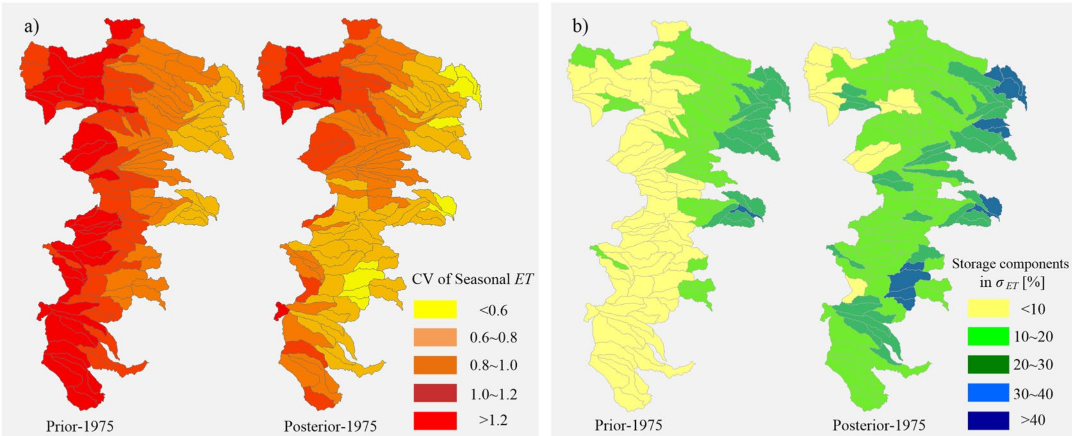

Figure 4. (a) The coefficient of variation (CV) of *ET* seasonal variability and (b) the percentage of storage components in σ^2_{ET} (i.e., the sum of groundwater components $w_{\Delta S}\sigma^2_{\Delta S} + w_{P,\Delta S}cov_{P,\Delta S} + w_{PET,\Delta S}cov_{PET,\Delta S}$ over the total σ^2_{ET} in Equation 2).

sub-basins in the east. However, more erratic spatial heterogeneity is seen in σ_{ET} post-1975 shown in the right map of Figure 3b. Despite a common decrease in σ_{ET} climatic components, the increase of σ_{ET} storage components at some locations causes the spatial heterogeneity, especially in the Republican River Basin in the NHP and some sub-basins in the CHP and SHP. The east-to-west gradient in σ_{ET} only remains in the north part of the NHP, where groundwater pumping is negligible. The σ_{ET} estimated in Figures 2b and 3b with long records of seasonal groundwater level observation complements the estimation using the GRACE-derived terrestrial storage change (Zeng & Cai, 2018), providing a comparison of σ_{ET} change estimates due to extensive groundwater-based irrigation.

Change in *ET* mean and variance can be represented by the coefficient of variation (CV), a dimensionless indicator for relative variability. To be consistent in the temporal scale, *ET* seasonal variance is normalized by the mean seasonal *ET* (i.e., half of the mean annual *ET*). Similar to the mean and variance, the CV of seasonal *ET* pre-1975 in the left of Figure 4a displays an apparent east-to-west gradient with lower CV in the east sub-basins and higher CV in the west sub-basins. However, the spatial gradient is not preserved post-1975, except for in the north part of the NHP in Figure 4b. There is a consistent decrease in CV in most sub-basins in the south parts of the NHP, CHP, and SHP. Although some sub-basins have increased σ_{ET} due to irrigation, the increase in mean *ET* is more significant. Therefore, irrigation dampens *ET* variability in term of CV, while as shown above, irrigation increases the absolute value of variability (σ_{ET}). Some sub-basins in the CHP and east part of the NHP have CVs lower than 0.6, which is not observed pre-1975.

3.3. The Sources of σ_{ET} Change

As discussed above, changes in climate and groundwater-fed irrigation are the two main sources of σ_{ET}. Figure 2b illustrates the percentage of storage components (i.e., $w_{\Delta S}\sigma^2_{\Delta S} + w_{P,\Delta S}cov_{P,\Delta S} + w_{PET,\Delta S}cov_{PET,\Delta S}$) in total σ^2_{ET}. Note that since the components from storage change can be negative, the percentage is calculated using the absolute values. Before 1975, the storage components account for less than 10% of σ_{ET} in most sub-basins of the CHP and SHP. The east part of the NHP has a higher portion (about 20%) with the storage components than the west part (less than 10%). After 1975, there is a significant increase in the storage components of σ_{ET}: Most sub-basins have more than 10% and some have even more than 40%. Sub-basins with contribution from storage components higher than 20% are distributed unevenly, showing spatial heterogeneity (the left map of Figure 2b). The groundwater fluctuation ($\sigma_{\Delta S}$) and pumping response to rainfall deficit ($cov_{P,\Delta S}$) increase the contribution of storage components to σ_{ET}. The spatial heterogeneity caused by irrigation is also reflected by storage components in σ_{ET} in the right map in Figure 4b. Thus, compared to the climatic components, the anthropogenic induced storage components play a notable role in shaping the *ET* variability in this region. A higher storage component in σ_{ET} represent a closer coupling between land surface processes and groundwater dynamics due to agricultural development.

4. Discussion

4.1. The Overlapping of Natural Gradients and Anthropogenic-Induced Heterogeneity in ET

The spatial characteristics in the High Plains under natural conditions exhibit a clear east-to-west gradient. Due to the rising terrain toward the west, *P* decreases from east to west (Daly et al., 2008). The regional water table under the "pre-development" condition (or the near natural condition) also follows the east-to-west gradient (Haacker et al., 2016; McGuire, 2014). The north-to-south gradient of *PET* (following the temperature gradient) does not manifest in the hydroclimatic spatial pattern in the arid and semi-arid climate, since the land surface processes in this region are constrained by *P*. The *ET* characteristics, including the mean, seasonal variance, seasonal CV and storage components, also show an apparent east-to-west gradient pre-1975. Natural vegetation or rain-fed crops depend on soil moisture to buffer the climatic fluctuation and have limited accessibility to groundwater. Therefore, the *ET* in the region pre-1975 was mainly affected by the climate, and its spatial pattern followed the east-to-west climatic gradient. With substantial groundwater-fed irrigation development, localized groundwater depletion propagates to *ET* pattern changes and introduces anthropogenic spatial heterogeneity over the natural east-to-west gradient, as shown by the post-1975 maps of Figures 2–4. As anthropogenic-induced storage components in σ_{ET} became significant, the hydrologic system in the High Plains went beyond a "natural" system that was driven by climate forcings, to one that is now driven by both natural (climatic, geomorphic) and anthropogenic (e.g., land use and water withdrawals) factors. The High Plains has been shifted from a natural system to a CHNS with extensive irrigation development in the region. This study provides an observational evidence of ET spatial and temporal changes due to extensive groundwater-fed irrigation. However, to quantify the contribution of various hydrologic processes (e.g., climate change) and human activities to ET change in this region with confirmed statistical significance, more systematic designed numerical experiments are needed to represented the irrigation scheme (e.g., when, where and how irrigation water are applied to the field).

The anthropogenic-induced *ET* heterogeneity in the High Plains highlights an indispensable issue in understanding hydrologic systems in the context of a CHNS, where the natural east-to-west gradient and anthropogenic-induced heterogeneity jointly shape the spatial pattern of *ET*. Our understanding of natural dynamics and capability to predict hydroclimatic changes have been fundamentally improved by observations across different spatial scales and spatially-distributed simulation models. The advances in data acquisition and model improvement enable earth scientists to explore the complexity of natural processes, which further supports and strengthens scientific-based decision-making on water resources development. However, the spatial heterogeneity on the human dimension is less well established in either the data or modeling aspects (Xu et al., 2014). Traditional water resources planning and management models generally adopt a simplified top-down and homogenous institution and overlook the heterogeneity in human behaviors (Yang et al., 2009). As evidenced in the *ET* pattern change in the High Plains, anthropogenic-induced *ET* components show even stronger heterogeneity than the natural gradient due to spatially diversified irrigation practices resulting from human behaviors. An individual farmers' irrigation decisions are affected by spatially distributed environmental conditions (Noël & Cai, 2017), groundwater management policy (Hrozencik et al., 2017) and the farmer's response to weather forecasts (Hejazi et al., 2014). Further, Foster et al. (2014) found that irrigation behavior in Texas High Plains region exhibits complex nonlinear responses to changes in groundwater availability and well yield. Below the state level, groundwater-management authorities, such as Natural Resources Districts with the State of Nebraska, monitor groundwater usage and in some cases regulate farmers' allowable pumping volume. At the interstate level, water rights conflicts are settled by the Republican River Compact Administration, which allocates the water rights of the Republican River among Colorado, Kansas and Nebraska (Draper, 2007). These cross-scale anthropogenic complexities require a new modeling paradigm to incorporate institutionally-sound and behaviorally-realistic decision mechanisms to support the modeling of CHNS (Vogel et al., 2015). Emerging concepts, such as of socio-hydrology (Sivapalan et al., 2012) and hydro-geomorphology (Vogel, 2011), and the "bottom-up" approach in agent-based modeling (Bitterman & Koliba, 2020; Ng et al., 2011; Noël & Cai, 2017), provide promising guidelines toward strengthening the human dimension in CHNS.

4.2. Correspondence Between *ET* Pattern and Crop Production

ET processes occur within the context of crop production management for both irrigated and rain-fed agriculture. Thus, the pattern of *ET* change can help unveil crop production variability. Figure 5a shows the evolution of *ET* pattern for the 120 sub-basins for the periods pre- and post-1975. The pairwise points (pre- and post-1975) in each sub-basin generally shift from upper-left (high CV and low mean) to lower-right (low CV and high mean)

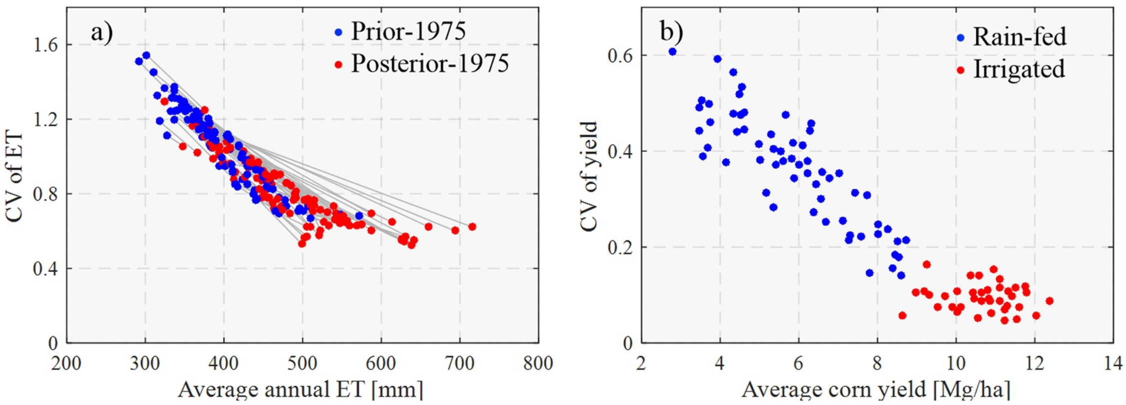

Figure 5. (a) Annual average *ET* versus CV for the 120 sub-basins in the High Plains, pre-1975 and post-1975; (b) average versus CV of rain-fed and irrigated corn yields in Nebraska.

as substantial groundwater pumping has developed over the region. Therefore, irrigation alters two aspects of crop water consumption by (a) increasing the mean crop water consumption (in order to mitigate the deficit in rainfall) and (b) damping the variation of crop water consumption (in order to buffer the climatic fluctuation). We may make an analogy between crop water consumption and crop yield by showing a similar pattern observed for crop yield as shown in Figure 5b, the rain-fed and irrigated corn yield in Nebraska based on data from the United States Department of Agriculture National Agricultural Statistics Service. The rain-fed corn yield has high CV and low mean, and the irrigated corn yield exhibits low CV and high mean, corresponding to high mean and low variance of *ET* with irrigated corn and low mean and high variance of *ET* with rain-fed corn. Note that due to the data availability, the corn yield is summarized at the county level. It would be ideal to show the crop yield at sub-basin level corresponding to the ET data. The analogy between ET and crop yield in Figure 5 provides a testable hypothesis at the system level, which can be further cross-validated with processed-based land surface models, statistical downscaling or integrated surface-and groundwater models.

The correspondence between *ET* pattern (a natural process variable) and crop yield (an anthropogenic variable) manifests as an emerging phenomenon of CHNS in the High Plains, as the nature and human components are coupled closely. Comparing the crop yield as farmers' profit and crop yield CV as the risk over time, the transition from high-CV-and-low-mean to low-CV-and-high-mean in Figure 5b shows that irrigation has turned the crop system into a state favorable to farmers (higher profit and lower risk than those from rain-fed crops). Meanwhile, *ET* pattern change (Figure 5a) reflects a hydroclimatic state shift from a natural condition to managed condition. However, the *ET* change has been accompanied by some "unintended" environmental consequences, that is, water table drawdown and stream depletion in the region (Haacker et al., 2016; Konikow & Kendy, 2005; Scanlon, Faunt, et al., 2012) as shown in Figure 6 and Figure S3 in Supporting Information S1. It is noted that streamflow declines in this region are observed mostly in upstream rivers (with small annual discharge) because of baseflow reduction, while downstream rivers (with large annual discharge) remain relatively stable. It is possible that irrigation return flow from in the upstream may partially compensate the baseflow decline.

An equilibrium state of the CHNS is associated with tradeoff between agricultural profit and environmental sustainability; upon reaching a tipping point, the tradeoff can cause a state shift of both nature and human systems toward a new equilibrium of the CHNS. For example, the 2002 Supreme Court final settlement on the Republican River Basin water allocation conflict between downstream Kansas and upstream Colorado and Nebraska ended with more limited pumping permits for farmers in the upstream states, especially for those who had irrigated land along the river. The pumping permit reduces from 20 inches in the 1980s to 13.5 inches at present (Kuwayama & Brozović, 2013). The regulation changes have limited the groundwater pumping for irrigation, prevented water depletion, and restored the streamflow to some extent (Smith et al., 2011). The USGS water use reports also shows that agricultural withdrawals in this region have peaked and started to decrease in recent years (Zeng & Ren, 2022).

Therefore, Figures 5 and 6 provides a linkage among climatic fluctuation, engineering and socioeconomic measures, crop yield, and environmental change (i.e., water table change) in the context of CHNS. Farmers need to hedge their income risk against the climatic variability if groundwater pumping permit is further restricted, and institutional change might be needed (e.g., on crop insurance) to protect farmers' income. The

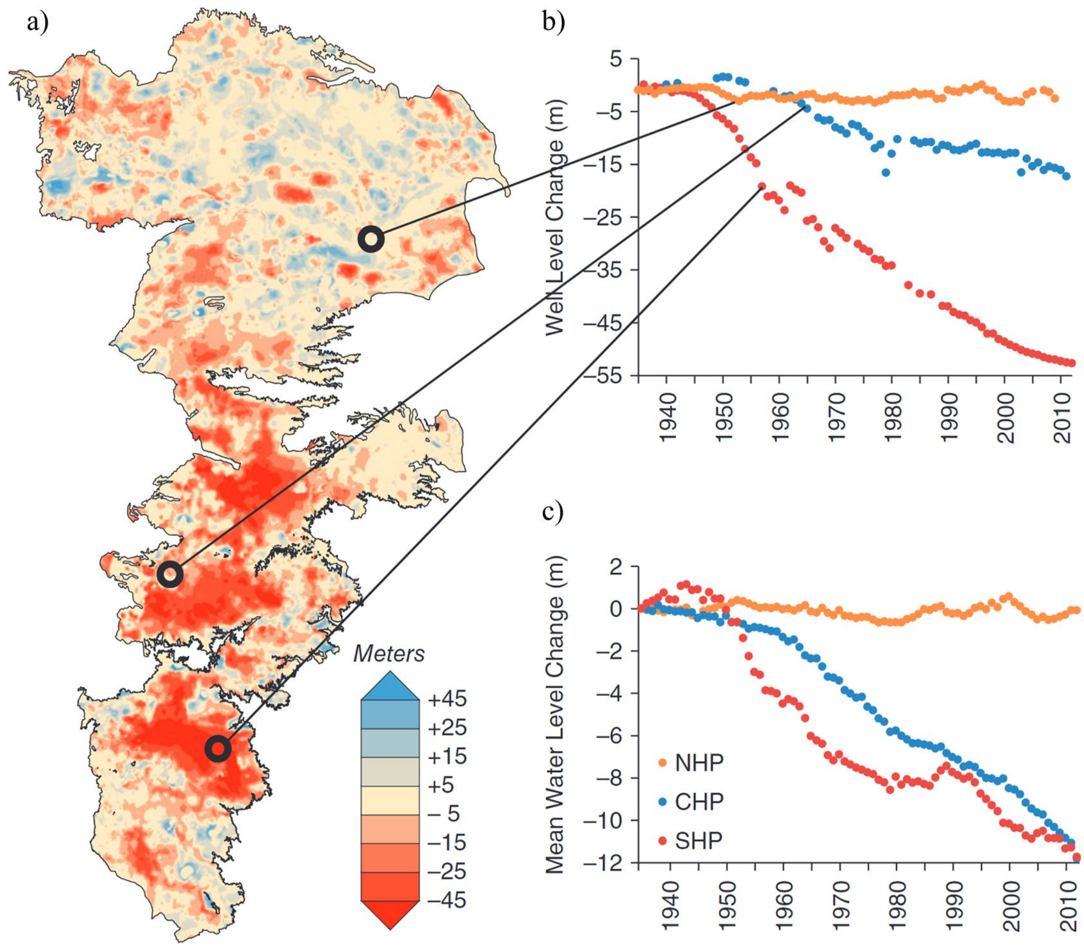

Figure 6. (a) Water level change, from the predevelopment surface to 2012. (b) Hydrographs of individual wells from each of the regions of the High Plains (USGS site IDs: SHP, 341420101441602; CHP, 362746102364102; NHP, 404345098560001). (c) Average water level change across the three regions of the High Plains. SHP, CHP, NHP stand for Southern, Central, and Northern High Plains respectively. Adapted from Haacker et al. (2016).

relationship between *ET* mean (related to crop yield) and CV (crop yield fluctuation) provides fundamental information for agricultural insurance policies designed to buffer against natural fluctuations (Glauber, 2004; Schurle, 1996).

5. Conclusion

Extensive groundwater pumping for irrigation has caused groundwater storage and streamflow depletion in the High Plains. To address such a concern of sustainability, this study assesses changes in *ET* spatial-temporal patterns in the High Plains region using climate and water table observations starting from 1940 and Evapotranspiration Temporal VARiance Decomposition (ETVARD) framework, a tool to compute the inter-period *ET* variance. By comparing the *ET* patterns pre-1975 and post-1975, we find that, on average, groundwater pumping contributes about 39.1 mm to the total 74.1 mm increase in *ET*, while precipitation contributes about 35.0 mm. The decrease in seasonal σ_{ET} is mainly due to the decline in climatic components (20.7 mm) and offset by the increase from storage components (14.2 mm), indicating a buffering effect of groundwater fed irrigation on ET variability. In terms of magnitude, groundwater-fed irrigation accounts for 41% of changes in σ_{ET} after 1975. The substantial magnitude of groundwater irrigation makes the anthropogenic components in σ_{ET} comparable to the climatic factors. Before 1975, the *ET* spatial pattern exhibits a clear east-to-west gradient following the natural (e.g., terrain and *P*) gradient. After 1975, anthropogenic-induced heterogeneity overrides the natural east-to-west gradient due to localized groundwater pumping, which has been caused by the various hierarchical institutional factors such as regional water rights, regulation by local natural resources authorities, and individual farmer's preferences.

We further show a statistical correspondence between the mean and CV of *ET* and those of crop yield, illustrating an analogy between *ET* change and crop production. Such a correspondence manifests the coupling of the hydroclimatic and anthropogenic components in the High Plains. The tradeoff of agriculture production and environmental integrity affects the stability of the CHNS, and appropriate policies (e.g., regulations on pumping, financial incentives, and farmers' preferences on risk) may shift the system to a more sustainable state.

Appendix A: Derivation of Short-Term Variability Impacts on Mean *ET*

Taylor expansion of Equation 4 near the long-term average climate condition (i.e., $\overline{P}, \overline{PET}$, the overbar denotes long-term average) by neglecting high order terms is:

$$\begin{aligned} ET_i = {} & f\left(\overline{P}, \overline{PET}, \overline{\Delta S}\right) + f'_P\left(\overline{P}, \overline{PET}, \overline{\Delta S}\right)\left(P_i - \overline{P}\right) + f'_{PET}\left(\overline{P}, \overline{PET}, \overline{\Delta S}\right)\left(PET_i - \overline{PET}\right) \\ & + f'_{\Delta S}\left(\overline{P}, \overline{PET}, \overline{\Delta S}\right)\left(\Delta S_i - \overline{\Delta S}\right) + \frac{1}{2!}\left[f''_P\left(\overline{P}, \overline{PET}, \overline{\Delta S}\right)\left(P_i - \overline{P}\right)^2\right. \\ & + f''_{PET}\left(\overline{P}, \overline{PET}, \overline{\Delta S}\right)\left(PET_i - \overline{PET}\right)^2 + f''_{\Delta S}\left(\overline{P}, \overline{PET}, \overline{\Delta S}\right)\left(\Delta S_i - \overline{\Delta S}\right)^2 \\ & + 2f''_{P,\Delta S}\left(\overline{P}, \overline{PET}, \overline{\Delta S}\right)\left(P_i - \overline{P}\right)\left(\Delta S_i - \overline{\Delta S}\right) + 2f''_{PET,\Delta S}\left(\overline{P}, \overline{PET}, \overline{\Delta S}\right)\left(PET_i - \overline{PET}\right)\left(\Delta S_i - \overline{\Delta S}\right) \\ & \left. + 2f''_{P,PET}\left(\overline{P}, \overline{PET}, \overline{\Delta S}\right)\left(P_i - \overline{P}\right)\left(PET_i - \overline{PET}\right)\right] \end{aligned} \tag{A1}$$

where f'_X and f''_X represent the first- and second-order derivatives of Equation 1 with respect to the variable *X*.

When using Yang's expression for Budyko curve in Equation 2, the second order derivative terms in Equation 5 are:

$$\begin{aligned} f''_P &= (n-1)\left[(P-\Delta S)^n + PET^n\right]^{1/n-2}\left\{(P-\Delta S)^{n-2}\left[-(P-\Delta S)^n - PET^n\right] + (P-\Delta S)^{2n-2}\right\} \\ f''_{PET} &= -(n-1)PET^{n-2}(P-\Delta S)^n\left[(P-\Delta S)^n + PET^n\right]^{1/n-2} \\ f''_{\Delta S} &= (n-1)\left[(P-\Delta S)^n + PET^n\right]^{1/n-2}\left\{(P-\Delta S)^{n-2}\left[-(P-\Delta S)^n - PET^n\right] + (P-\Delta S)^{2n-2}\right\} \\ f''_{P,PET} &= nPET^{n-1}(P-\Delta S)^{n-1}\left[(P-\Delta S)^n + PET^n\right]^{1/n-2} \\ &\quad -PET^{n-1}(P-\Delta S)^{n-1}\left[(P-\Delta S)^n + PET^n\right]^{1/n-2} \\ f''_{P,\Delta S} &= (n-1)PET^n(P-\Delta S)^{n-2}\left[(P-\Delta S)^n + PET^n\right]^{1/n-2} \\ f''_{PET,\Delta S} &= PET^{n-1}(P-\Delta S)^{n-1}\left[(P-\Delta S)^n + PET^n\right]^{1/n-2} \\ &\quad -nPET^{n-1}(P-\Delta S)^{n-1}\left[(P-\Delta S)^n + PET^n\right]^{1/n-2} \end{aligned} \tag{A2}$$

Data Availability Statement

Historical precipitation and temperature are accessible from PRISM: https://prism.oregonstate.edu/historical/. The potential evaporation data is from NLDAS-2 forcing: https://ldas.gsfc.nasa.gov/data. Groundwater table change data is from Haacker et al. (2016) https://ngwa.onlinelibrary.wiley.com/doi/full/10.1111/gwat.12350. Crop yield data is retrieved from USDA National Agricultural Statistics Service: https://quickstats.nass.usda.gov/. The data processed by this study can be accessed from Hydroshare: http://www.hydroshare.org/resource/fd217ef73ce04962acf45c8845a8e0d6.

Acknowledgments

R. Zeng is supported by NOAA COM Grant NA20OAR4310341. Haacker's research was supported by National Science Foundation Award WSC 1039180. The authors appreciate the constructive comments and suggestions from the editor, associate editor and reviewers.

References

Aeschbach-Hertig, W., & Gleeson, T. (2012). Regional strategies for the accelerating global problem of groundwater depletion. *Nature Geoscience*, *5*(12), 853–861. https://doi.org/10.1038/ngeo1617

Bitterman, P., & Koliba, C. J. (2020). Modeling alternative collaborative governance network designs: An agent-based model of water governance in the Lake Champlain Basin, Vermont. *Journal of Public Administration Research and Theory*, *30*(4), 636–655. https://doi.org/10.1093/jopart/muaa013

Burt, O. R., Baker, M., & Helmers, G. A. (2002). Statistical estimation of streamflow depletion from irrigation wells. *Water Resources Research*, *38*(12), 1296. https://doi.org/10.1029/2001WR000961

Daly, C., Halbleib, M., Smith, J. I., Gibson, W. P., Doggett, M. K., Taylor, G. H., et al. (2008). Physiographically sensitive mapping of climatological temperature and precipitation across the conterminous United States. *International Journal of Climatology*, *28*(15), 2031–2064. https://doi.org/10.1002/joc.1688

Demissie, Y., Valocchi, A., Cai, X., Brozovic, N., Senay, G., & Gebremichael, M. (2015). Parameter estimation for groundwater models under uncertain irrigation data. *Groundwater*, *53*(4), 614–625. https://doi.org/10.1111/gwat.12235

Dieter, C. A., & Maupin, M. A. (2017). *Public supply and domestic water use in the United States, 2015 (No. 2017-1131)*. US Geological Survey.

Draper, S. E. (2007). Administration and institutional provisions of water sharing agreements. *Journal of Water Resources Planning and Management*, *133*(5), 446–455. https://doi.org/10.1061/(ASCE)0733-9496(2007)133:5(446)

Famiglietti, J. S. (2014). The global groundwater crisis. *Nature Climate Change*, *4*(11), 945–948. https://doi.org/10.1038/nclimate2425

Foster, S., & Garduño, H. (2004). *Towards sustainable groundwater resource use for irrigated agriculture on the North China Plain*. World Bank.

Foster, T., Brozović, N., & Butler, A. P. (2014). Modeling irrigation behavior in groundwater systems. *Water Resources Research*, *50*(8), 6370–6389. https://doi.org/10.1002/2014WR015620

Fu, B. (1981). On the calculation of the evaporation from land surface (in Chinese). *Scientia Atmospherica Sinica*, *5*(1), 23–31.

Glauber, J. W. (2004). Crop insurance reconsidered. *American Journal of Agricultural Economics*, *86*(5), 1179–1195. https://doi.org/10.1111/j.0002-9092.2004.00663.x

Green, D. E. (1981). *Land of the underground rain: Irrigation on the Texas High Plains*, 1910-1970. University of Texas Press.

Gutentag, E. D. (1984). Geohydrology of the High Plains aquifer in parts of Colorado, Kansas, Nebraska, New Mexico, Oklahoma, South Dakota, Texas, and Wyoming. In *Geological Survey professional paper, 1400-B*.

Haacker, E. M., Kendall, A. D., & Hyndman, D. W. (2016). Water level declines in the High Plains Aquifer: Predevelopment to resource senescence. *Groundwater*, *54*(2), 231–242. https://doi.org/10.1111/gwat.12350

Han, S., Hu, H., Yang, D., & Liu, Q. (2011). Irrigation impact on annual water balance of the oases in Tarim Basin, Northwest China. *Hydrological Processes*, *25*(2), 167–174. https://doi.org/10.1002/hyp.7830

Hargreaves, G. H., & Samani, Z. A. (1982). Estimating potential evapotranspiration. *Journal of the Irrigation and Drainage Division*, *108*(3), 225–230. https://doi.org/10.1061/jrcea4.0001390

Hejazi, M., Cai, X., Yuan, X., Liang, X., & Kumar, P. (2014). Incorporating reanalysis-based short-term forecasts from a regional climate model in an irrigation scheduling optimization problem. *Journal of Water Resources Planning and Management*, *140*(5), 699–713. https://doi.org/10.1061/(ASCE)WR.1943-5452.0000365

Hornbeck, R., & Keskin, P. (2014). The historically evolving impact of the ogallala aquifer: Agricultural adaptation to groundwater and drought. *American Economic Journal: Applied Economics*, *6*(1), 190–219. https://doi.org/10.1257/app.6.1.190

Hrozencik, R. A., Manning, D. T., Suter, J. F., Goemans, C., & Bailey, R. T. (2017). The heterogeneous impacts of groundwater management policies in the Republican River Basin of Colorado. *Water Resources Research*, *53*(12), 10757–10778. https://doi.org/10.1002/2017wr020927

Istanbulluoglu, E., Wang, T., Wright, O. M., & Lenters, J. D. (2012). Interpretation of hydrologic trends from a water balance perspective: The role of groundwater storage in the Budyko hypothesis. *Water Resources Research*, *48*(3), W00H16. https://doi.org/10.1029/2010WR010100

Joodaki, G., Wahr, J., & Swenson, S. (2014). Estimating the human contribution to groundwater depletion in the Middle East, from GRACE data, land surface models, and well observations. *Water Resources Research*, *50*(3), 2692. https://doi.org/10.1002/2013WR014633

Konikow, L., & Kendy, E. (2005). Groundwater depletion: A global problem. *Hydrogeology Journal*, *13*(1), 317–320. https://doi.org/10.1007/s10040-004-0411-8

Konikow, L. F. (2011). Contribution of global groundwater depletion since 1900 to sea-level rise. *Geophysical Research Letters*, *38*(17), L17401. https://doi.org/10.1029/2011GL048604

Kuwayama, Y., & Brozović, N. (2013). The regulation of a spatially heterogeneous externality: Tradable groundwater permits to protect streams. *Journal of Environmental Economics and Management*, *66*(2), 364–382. https://doi.org/10.1016/j.jeem.2013.02.004

Lawston, P. M., Santanello, J. A., Jr., Zaitchik, B. F., & Rodell, M. (2015). Impact of irrigation methods on land surface model spinup and initialization of WRF forecasts. *Journal of Hydrometeorology*, *16*(3), 1135–1154. https://doi.org/10.1175/jhm-d-14-0203.1

Liu, J., Dietz, T., Carpenter, S. R., Alberti, M., Folke, C., Moran, E., et al. (2007). Complexity of coupled human and natural systems. *Science*, *317*(5844), 1513–1516. https://doi.org/10.1126/science.1144004

Liu, J., Zheng, C., Zheng, L., & Lei, Y. (2008). Ground water sustainability: Methodology and application to the North China Plain. *Ground Water*, *46*(6), 897–909. https://doi.org/10.1111/j.1745-6584.2008.00486.x

Mahrt, L., & Ek, M. (1984). The influence of atmospheric stability on potential evaporation. *Journal of Climate and Applied Meteorology*, *23*(2), 222–234. https://doi.org/10.1175/1520-0450(1984)023<0222:TIOASO>2.0.CO;2

McGuire, V. L. (2009). Changes in water levels and storage in the High Plains aquifer, predevelopment to 2007.

McGuire, V. L. (2014). *Water-level changes and change in water in storage in the High Plains aquifer, predevelopment to 2013 and 2011–2013* (p. 14). U.S. Geological Survey Scientific Investigations Report 2014 - 5218. https://doi.org/10.3133/sir20145218

McGuire, V. L., Lund, K. D., & Densmore, B. K. (2012). *Saturated thickness and water in storage in the High Plains aquifer, 2009, and water-level changes and changes in water in storage in the High Plains aquifer, 1980 to 1995, 1995 to 2000, 2000 to 2005, and 2005 to 2009* (p. 2028). U.S. Geological Survey Scientific Investigations Report, 2012-5177. Retrieved from http://pubs.usgs.gov/sir/2012/5177/

Mutiibwa, D., & Irmak, S. (2013). AVHRR-NDVI-based crop coefficients for analyzing long-term trends in evapotranspiration in relation to changing climate in the U.S. High Plains. *Water Resources Research*, *49*(1), 231–244. https://doi.org/10.1029/2012WR012591

Ng, T. L., Eheart, J. W., Cai, X., & Braden, J. B. (2011). An agent-based model of farmer decision-making and water quality impacts at the watershed scale under markets for carbon allowances and a second-generation biofuel crop. *Water Resources Research*, *47*(9), W09519. https://doi.org/10.1029/2011WR010399

Noël, P. H., & Cai, X. (2017). On the role of individuals in models of coupled human and natural systems: Lessons from a case study in the Republican River Basin. *Environmental Modelling & Software*, *92*, 1–16. https://doi.org/10.1016/j.envsoft.2017.02.010

Ozdogan, M., Rodell, M., Beaudoing, H. K., & Toll, D. L. (2010). Simulating the effects of irrigation over the United States in a land surface model based on satellite-derived agricultural data. *Journal of Hydrometeorology*, *11*(1), 171–184. https://doi.org/10.1175/2009JHM1116.1

Popelka, A. M. (2004). The Republican River dispute: An analysis of the parties' compact interpretation and final settlement stipulation. *Nebraska Law Review*, *83*, 596.

Rodell, M., Velicogna, I., & Famiglietti, J. S. (2009). Satellite-based estimates of groundwater depletion in India. *Nature*, *460*(7258), 999–1002. https://doi.org/10.1038/nature08238

Rossman, N. R., & Zlotnik, V. A. (2013). Review: Regional groundwater flow modeling in heavily irrigated basins of selected states in the western United States. *Hydrogeology Journal*, *21*(6), 1173–1192. https://doi.org/10.1007/s10040-013-1010-3

Scanlon, B. R., Faunt, C. C., Longuevergne, L., Reedy, R. C., Alley, W. M., McGuire, V. L., & McMahon, P. B. (2012). Groundwater depletion and sustainability of irrigation in the US High Plains and Central Valley. *Proceedings of the National Academy of Sciences of the United States of America*, *109*(24), 9320–9325. https://doi.org/10.1073/pnas.1200311109

Scanlon, B. R., Longuevergne, L., & Long, D. (2012). Ground referencing GRACE satellite estimates of groundwater storage changes in the California Central Valley, USA. *Water Resources Research*, *48*(4), W04520. https://doi.org/10.1029/2011WR011312

Schurle, B. (1996). The impact of size on yield variability and crop insurance premiums. *Review of Agricultural Economics*, *18*(3), 415–422. https://doi.org/10.2307/1349625

Seaber, P. R., Kapinos, F. P., & Knapp, G. L. (1987). *Hydrologic unit maps*. U.S. Geological Survey, Water Supply Paper 2294.

Sivapalan, M., Savenije, H. H. G., & Blöschl, G. (2012). Socio-hydrology: A new science of people and water. *Hydrological Processes*, *26*(8), 1270–1276. https://doi.org/10.1002/hyp.8426

Smith, L. M., Haukos, D. A., McMurry, S. T., LaGrange, T., & Willis, D. (2011). Ecosystem services provided by playas in the High Plains: Potential influences of USDA conservation programs. *Ecological Applications*, *21*(sp1), S82–S92. https://doi.org/10.1890/09-1133.1

Strassberg, G., Scanlon, B. R., & Chambers, D. (2009). Evaluation of groundwater storage monitoring with the GRACE satellite: Case study of the High Plains aquifer, central United States. *Water Resources Research*, *45*(5), W05410. https://doi.org/10.1029/2008WR006892

Szilagyi, J. (1999). *Streamflow depletion investigations in the Republican River Basin: Colorado*. Nebraska, and Kansas.

Szilagyi, J. (2001). Identifying cause of declining flows in the Republican River. *Journal of Water Resources Planning and Management*, *127*(4), 244–253. https://doi.org/10.1061/(ASCE)0733-9496(2001)127:4(244)

Szilagyi, J., & Franz, T. E. (2020). *Anthropogenic hydrometeorological changes at a regional scale: Observed irrigation–precipitation feedback (1979–2015) in Nebraska, USA* (Vol. 6, pp. 1–10). Sustainable Water Resources Management.

Vogel, R. (2011). Hydromorphology. *Journal of Water Resources Planning and Management*, *137*(2), 147–149. https://doi.org/10.1061/(ASCE)WR.1943-5452.0000122

Vogel, R. M., Lall, U., Cai, X., Rajagopalan, B., Weiskel, P. K., Hooper, R. P., & Matalas, N. C. (2015). Hydrology: The interdisciplinary science of water. *Water Resources Research*, *51*(6), 4409–4430. https://doi.org/10.1002/2015WR017049

Wang, T., Istanbulluoglu, E., Lenters, J., & Scott, D. (2009). On the role of groundwater and soil texture in the regional water balance: An investigation of the Nebraska Sand Hills, USA. *Water Resources Research*, *45*(10), W10413. https://doi.org/10.1029/2009WR007733

Wei, S., Xu, T., Niu, G. Y., & Zeng, R. (2022). Estimating irrigation water consumption using machine learning and remote sensing data in Kansas high plains. *Remote Sensing*, *14*(13), 3004. https://doi.org/10.3390/rs14133004

Wen, F., & Chen, X. (2006). Evaluation of the impact of groundwater irrigation on streamflow in Nebraska. *Journal of Hydrology*, *327*(3–4), 603–617. https://doi.org/10.1016/j.jhydrol.2005.12.016

Xu, T., Valocchi, A. J., Choi, J., & Amir, E. (2014). Use of machine learning methods to reduce predictive error of groundwater models. *Groundwater*, *52*(3), 448–460. https://doi.org/10.1111/gwat.12061

Yang, D., Sun, F., Liu, Z., Cong, Z., Ni, G., & Lei, Z. (2007). Analyzing spatial and temporal variability of annual water-energy balance in nonhumid regions of China using the Budyko hypothesis. *Water Resources Research*, *43*(4), W04426. https://doi.org/10.1029/2006wr005224

Yang, H., Yang, D., Lei, Z., & Sun, F. (2008). New analytical derivation of the mean annual water-energy balance equation. *Water Resources Research*, *44*(3), W03410. https://doi.org/10.1029/2007wr006135

Yang, Y.-C. E., Cai, X., & Stipanović, D. M. (2009). A decentralized optimization algorithm for multiagent system–based watershed management. *Water Resources Research*, *45*(8), W08430. https://doi.org/10.1029/2008WR007634

Zeng, R., & Cai, X. (2014). Analyzing streamflow changes: Irrigation-enhanced interaction between aquifer and streamflow in the Republican River Basin. *Hydrology and Earth System Sciences*, *18*(2), 493–502. https://doi.org/10.5194/hess-18-493-2014

Zeng, R., & Cai, X. (2015). Assessing the temporal variance of evapotranspiration considering climate and catchment storage factors. *Advances in Water Resources*, *79*(0), 51–60. https://doi.org/10.1016/j.advwatres.2015.02.008

Zeng, R., & Cai, X. (2016). Climatic and terrestrial storage control on evapotranspiration temporal variability: Analysis of river basins around the world. *Geophysical Research Letters*, *43*(1), 185–195. https://doi.org/10.1002/2015GL066470

Zeng, R., & Cai, X. (2018). Hydrologic observation, model, and theory congruence on evapotranspiration variance: Diagnosis of multiple observations and land surface models. *Water Resources Research*, *54*(11), 9074–9095. https://doi.org/10.1029/2018wr022723

Zeng, R., & Ren, W. (2022). The spatiotemporal trajectory of US agricultural irrigation withdrawal during 1981–2015. *Environmental Research Letters*, *17*(10), 104027. https://doi.org/10.1088/1748-9326/ac91e2

Zhang, L., Dawes, W. R., & Walker, G. R. (2001). Response of mean annual evapotranspiration to vegetation changes at catchment scale. *Water Resources Research*, *37*(3), 701–708. https://doi.org/10.1029/2000wr900325

Zipper, S. C., Dallemagne, T., Gleeson, T., Boerman, T. C., & Hartmann, A. (2018). Groundwater pumping impacts on real stream networks: Testing the performance of simple management tools. *Water Resources Research*, *54*(8), 5471–5486. https://doi.org/10.1029/2018wr022707